# A quantum chemical study of the ground state ring opening/closing of photochromic 1,3,3-trimethylspiro[indoline-2,3′-naphtho[2,1-*b*]-[1,4]oxazine]

**François Maurel,*[a] Jean Aubard,[a] Michel Rajzmann,[b] Robert Guglielmetti[b] and André Samat[b]**

[a] *ITODYS, Université de Paris 7 – Denis Diderot, UMR CNRS 7086, 1 rue Guy de la Brosse, 75005 Paris, France*
[b] *LCMOM, Université de la Méditerranée, UMR CNRS 6114, Faculté des Sciences de Luminy, 13288 Marseille Cedex 9, France*

***Received (in Cambridge, UK) 12th March 2002, Accepted 1st May 2002***
***First published as an Advance Article on the web 27th May 2002***

Ground state ring opening/closing reactions of 1,3,3-trimethylspiro[indoline-2,3′-naphtho[2,1-*b*][1,4]oxazine] have been studied using DFT calculations. An extensive description of the ground state ring opening/closing and isomerization processes undergone by the eight open forms is proposed. The pathways for ring opening show that the most stable merocyanines, TTC and CTC, can be obtained after C–O bond cleavage of the (*R*)- and (*S*)-enantiomeric closed forms, respectively. Two s-*cis* isomers, CCC and TCC, were localized on the potential energy surface and characterized as key intermediates involved in the two previous pathways. The less stable merocyanines, CTT and TTT, revert to the corresponding closed form through an inversion mechanism at the N1′ nitrogen atom. This mechanism is suggested to explain the fast component of the kinetics of the thermal fading reaction. The ground state reaction of enantiomerization between the closed forms (*R*) and (*S*) is also reported and two competing mechanisms were found. Enantiomerization can be achieved by after ring opening by *cis–trans* isomerization either between two merocyanines (*i.e.* TTC and CTC) or two s-*cis* intermediates. The high energy barrier of the bond rotation necessary for the interconversion between TTC and CTC isomers makes this process less favorable than direct interconversion between the s-*cis* intermediates (CCC and TCC).

## 1 Introduction

Photochromism of organic compounds is defined as a reversible transformation, induced by light in one or both directions, between two states (A and B) which absorb light in different regions.[1,2]

$$A(\lambda_1) \underset{h\nu_2 \text{ or } \Delta}{\overset{h\nu_1 \text{ or } \Delta}{\rightleftharpoons}} B(\lambda_2) \qquad (1)$$

Among photochromic compounds, spirooxazines (SO) have received increasing interest during the past 20 years because of their good photochromic properties and light fatigue resistance.[3,4] Therefore, SO are currently used in many commercial applications, such as ophthalmic lenses, sunglasses,[5] memories and switches.[6] These compounds consist of two heterocyclic moieties linked together by an $sp^3$ spiro carbon atom (Scheme 1).

Absorption of UV light and/or temperature increase (thermochromism[7]) causes cleavage of the relatively weak spiro carbon–oxygen bond followed by conformational rearrangements, leading finally to ring-opened coloured isomers, the so-called photomerocyanines. The photomerocyanine species revert to the closed form through a thermally induced ring-closure reaction (Scheme 1); fading of the coloured forms occurs on a timescale of seconds to minutes at room temperature.[7] Obviously, the main properties of spironaphthoxazines, such as their quantum yields of photocolouration and their kinetics of ring closure, are determined by the features of both the ground and lowest excited states. Thus, detailed knowledge of these states along with the ring opening/closing mechanism should be useful for the rational design of new photochromic compounds with improved performances. In this paper we restrict our study to the ground state surface. The ground state

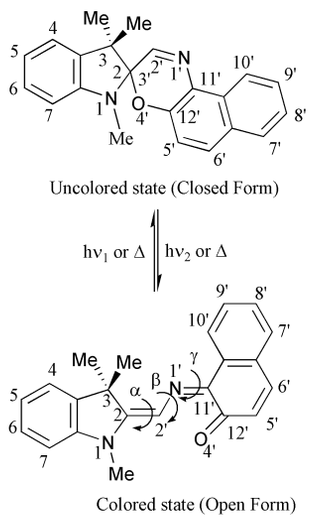


**Scheme 1**

mechanism for the opening/closing process is, however, complicated due to the existence of several open-form isomers and their interconversion. Many experimental studies have been undertaken to elucidate the photophysical and photochemical mechanisms. Because ring opening is an ultra-fast process, it has been studied almost exclusively using transient spectroscopies, and experimental studies of the ground state (thermochromic properties) are quite scarce. From time-resolved optical data and $^1H$ NMR spectroscopy, it has been shown that C–O bond cleavage results in the formation of mainly two merocyanine isomers having TTC and CTC structures (see Section 3.1.2 for the labeling of each merocyanine isomer). The amount of CTC is smaller than that of TTC. Several kinetic

DOI: 10.1039/b202545k

studies of the fading ring-closure reaction have shown that fading relaxation kinetics consists of at least two phases, suggesting that two or more isomers are involved in ring closure.[8] Recently, Mannschreck *et al.*[9] studied two thermal reactions of an asymmetric benzopyran–indoline photochromic compound. The first reaction was the transformation of the spiro form into the merocyanine, while the second was the interconversion of the two (*R*) and (*S*) spiro enantiomers. Both reactions should involve C–O bond cleavage but it was proposed that the transition states of C–O bond breaking for (*R*) and (*S*) are different, in order to take into account distinct mechanisms. Moreover, the interconversion of the enantiomeric closed forms (*R*) and (*S*) was suggested to occur through an achiral intermediate. However, experimental results did not demonstrate the existence of such an intermediate. Furthermore, it is difficult to imagine two different transition states involving the same C–O bond breaking. All these questions can be addressed by calculating the shape of the potential energy surface (PES) of the fundamental and first excited states that control the photocolouration and thermal fading reactions. Quantum chemical calculations are now recognized as useful tools in research related to the elucidation of molecular mechanisms. The understanding of a reaction mechanism at the molecular level for a given chemical reaction requires detailed knowledge of the stationary points on the PES: reactants, transition structures (TS), products, and possible intermediates. In particular, theoretical characterization of intermediates, TS and conical intersections provides a source of information, independent from experimental studies, concerning the geometry, electronic structure, and stereochemistry along the reaction pathway.[10] Despite their potential applications, few theoretical studies at the *ab initio* level of calculation have been performed on spirooxazines. Some authors have addressed the mechanism for spiropyrans and concluded that ring opening for such compounds occurs without any intermediate between the reactant and the merocyanine products.[11] However, the most relevant theoretical study on spironaphthoxazine by Nakamura *et al.*[12] focused on the relative thermodynamic stabilities of the four s-*trans* photomerocyanine isomers. The calculations indicated, in agreement with recent picosecond time-resolved Raman and vibrational analysis studies,[13] that the resonant species detected are s-*trans* planar forms with CTC and TTC geometries. All these studies give only a fragmentary mechanistic picture of the photochromism/thermochromism process and, despite the experimental improvement, neither experimental results nor calculations give a clear insight into the mechanism of photochromism in the spirooxazine series. In an attempt to highlight the thermal ring opening/closing reactions in this series, we report in this paper the lowest energy pathways for ground state ring closing of 1,3,3-trimethylspiro[indoline-2,3′-naphtho-[2,1-*b*][1,4]oxazine] (abbreviated in the following as spironaphthoxazine). The minima and the TS (Scheme 1) were characterized at the DFT level. In particular, this theoretical approach was focused on the question of the participation of a possible s-*cis* intermediate in the ring opening process and on the elucidation of ring closure for the merocyanine isomers.

## 2 Computational details

The choice of theoretical level depends on the accuracy required and the size of the molecule. Correlation energy corrections are always required for the calculation of reasonable activation energies, since correlation energy is often larger for transition structures than it is for stable molecules. Recent investigations have demonstrated that the DFT-B3LYP method leads to excellent results for geometries and energies.[14] Furthermore, this level of computation was found to take into account both localized structures, either quinoidal or zwitterionic, for merocyanine isomers (*vide infra*). Minima and transition state structures localized on the ground state potential energy surface (PES) were fully optimized without symmetry restrictions (convergence criteria = $10^{-4}$) with the B3LYP[15] density functional method and using the 3-21G basis set[16] (the integral grid used was fine). The Gaussian 94 program[17] was used for all DFT calculations. Vibrational frequencies were calculated at the same level of theory to characterize the optimized structures as a minimum or a first-order saddle point on the potential energy surface (the Hessian matrix revealed a single negative eigenvalue for each TS). Additional single point energy calculations were carried out with a larger basis set, *i.e.* 6-31G(d),[18] using the B3LYP/3-21G optimized geometries. To take into account solvent effects, energies were also computed at the B3LYP/6-31G(d) level with polarizable continuum solvation model calculations PCM[19] on B3LYP/3-21G geometries. In order to compare the theoretical calculations with the most significant experimental data, ethanol was chosen as solvent (relative permittivity $\varepsilon = 24.55$). Successfully completing a transition structure optimization does not guarantee that the right transition state has been found, *i.e.*, that which connects the reactants and products of interest and, therefore, we performed intrinsic reaction coordinate (IRC) calculations[20,21] to determine which minima a transition structure connects.

**Table 1** Calculated relative energies, $\Delta E$ (kcal mol$^{-1}$), and $\Delta G_{solvation}$ (kcal mol$^{-1}$) (in ethanol) of the closed and open forms of spironaphthoxazine (B3LYP/3-21G//3-21G and B3LYP/6-31G(d)//3-21G)

| | | B3LYP/3-21G | B3LYP/6-31G(d)//3-21G | |
|---|---|---|---|---|
| | Species | $\Delta E$ | $\Delta E$ | $\Delta G_{solvation}$ |
| | CF(R) | 0.0[a] | 0.0[b] | −7.2 |
| | CF(S) | 0.0 | 0.0 | −7.1 |
| s-*trans* | TTC | 5.2 | 2.8 | −4.2 |
| | CTC | 7.2 | 4.1 | −4.5 |
| | TTT | 15.3 | 12.7 | −5.2 |
| | CTT | 16.5 | 12.6 | −4.8 |
| s-*cis* | CCC | 18.6 | 15.5 | −4.2 |
| | TCC | 26.0 | 21.7 | −4.5 |
| | CCT | 30.9 | 25.5 | −7.8 |
| | TCT | 34.4 | 28.8 | −7.6 |

[a] −1029.441281 hartree. [b] −1035.112956 hartree.

## 3 Results and discussion

This section is divided in four subsections: thermodynamic and geometrical properties of the two closed and eight open forms (1); the interconversion of the coloured s-*trans* photomerocyanines in the ground state (2); ring-closure and thermochromic reactions (3 and 4, respectively).

### 3.1 Energies and geometries of closed and open forms

**3.1.1 Closed forms.** Due to the asymmetry of the spiro carbon atom, the closed form (CF) of spironaphthoxazine can exist as (*R*)- and (*S*)-enantiomers (Fig. 1), named as CF(R) and CF(S), respectively. These two enantiomeric forms have, of course, the same energy (Table 1). The geometrical parameters provided by the calculations are in good agreement with X-ray data[22] (Table 2). Except for the C2–O4′ bond, which is found to be slightly too long, the oxazine ring bond lengths are correctly reproduced by calculations (mean deviation of 0.02 Å). The C2–O4′ (1.500 Å) bond is longer than a normal C–O bond (1.41–1.43 Å) while the N1–C2 (1.456 Å) is shorter than normal N–C bonds (1.47–1.48 Å) in five-membered heterocycles. This effect is attributed to overlap between the lone pair orbital of N1 with the σ* orbital of the C2–O4′ bond.[23]

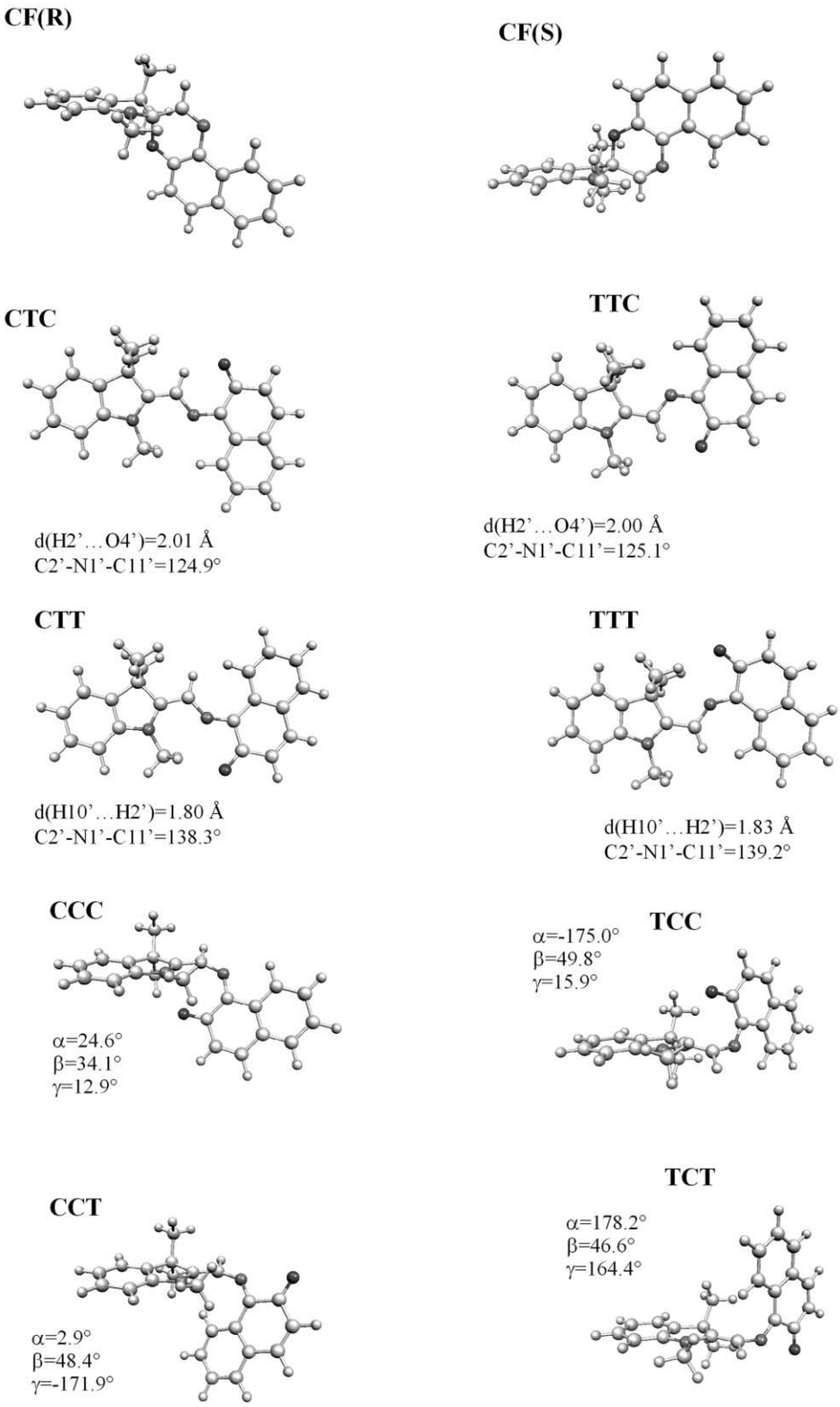


**Fig. 1** B3LYP/3-21G optimized geometries of the closed CF(R), CF(S) and of merocyanine isomers (s-*trans* and s-*cis*). See Scheme 1 for numbering of atoms.

**3.1.2 Open forms.** The open forms exhibit a central conjugated chain with three partial double bonds. Therefore, in principle, $2^3 = 8$ distinct isomers can be drawn. As already accepted by many authors,[12,24] each of these configurations can be labeled with a sequence of three letters C and/or T[24] indicating the approximate setting of the three dihedral angles $\alpha$, $\beta$ and $\gamma$ as *cis* ($0° < \beta < 90°$) or *trans* ($90° < \beta < 180°$), respectively (Scheme 1). Furthermore, isomers with a *trans* (*cis*) configuration with respect to the central C2′–N1′ bond will be named s-*trans* (s-*cis*). The relative energies of the open isomers are shown in Table 1. The TTC isomer is found to be the most stable open isomer (Table 1). Under thermodynamic control, the enthalpy of reaction, $\Delta H^0_{rxn}$, ($\Delta H^0_{rxn}$ is, as a first approximation, taken to be equal to $\Delta E$), is calculated to be *ca.* 2.8 kcal mol$^{-1}$ in the gas phase (B3LYP/6-31G(d)//3-21G) and 5.8 kcal mol$^{-1}$ in ethanol (PCM-B3LYP/6-31G(d)//3-21G). Although the gas phase value is not satisfactory compared with the experimental one in toluene (5.19 kcal mol$^{-1}$)[7,25] the ethanol value is in good agreement with experimental results (5.0 kcal mol$^{-1}$)[7,25] and supports the level of calculation. As previously

**Table 2** Selected parameters of the reactant, transition states, intermediate, and product going from CTC to CF(R) along the route **Ra** calculated at the B3LYP/3-21G level of theory

| Selected parameter[a,b] | CTC | TS(Rβ) | CCC | TS(R) | CF(R) Calc | CF(R) Exptl[c] |
|---|---|---|---|---|---|---|
| N1–C2 | 1.372 | 1.414 | 1.365 | 1.356 | 1.456 | 1.436 |
| C2–C2′ | 1.378 | 1.338 | 1.386 | 1.422 | 1.512 | |
| C2′–N1′ | 1.364 | 1.433 | 1.352 | 1.326 | 1.289 | |
| N1′–C11′ | 1.325 | 1.289 | 1.330 | 1.355 | 1.411 | 1.414 |
| C11′–C12′ | 1.486 | 1.528 | 1.480 | 1.451 | 1.384 | |
| C12′–O4′ | 1.262 | 1.244 | 1.266 | 1.288 | 1.382 | 1.362 |
| C2–O4′ | 4.049 | 3.187 | 2.602 | 2.271 | 1.500 | 1.454 |
| *α* | 0.0 | −1.2 | 24.6 | 48.3 | 109.8 | |
| *β* | 180.0 | 89.6 | 34.1 | 24.3 | 2.5 | |
| *γ* | 0.0 | 1.4 | 12.9 | 15.0 | 3.7 | |

[a] Distances in Å, angles in deg. [b] The atom numbering is shown in Scheme 1. [c] Ref. 22.

mentioned,[26] the s-*trans* isomers (TTC, CTC, TTT and CTT) are more stable by at least 10 kcal mol$^{-1}$ than the s-*cis* ones (CCC, TCC, CCT and TCT). Clearly, the s-*cis* isomers are less stable due to internal steric hindrance between the naphthalene and indoline moieties (Fig. 1). Under these conditions, the predicted relative thermodynamic stabilities are in the order: TTC < CTC < TTT < CTT < CCC < TCC < CCT < TCT, and this order remains practically unchanged in ethanol. The higher calculated stabilities for the TTC and CTC isomers, compared to the other isomers, are consistent with recent picosecond time-resolved resonance Raman spectroscopy[13] and NMR[27] studies. Since s-*cis* isomers are much less stable than s-*trans* isomers, this explains why these species have a very short life-time and can only be detected using very fast absorption spectroscopy with femtosecond resolution. However, since calculations suggest that the TTT and CTT isomers are more stable than the s-*cis* isomers, these species should be detected using this former technique. The geometries of the s-*trans* open forms are displayed in Fig. 1. All were found to be planar at the B3LYP/3-21G level of calculation. It is generally accepted that the geometry of such a conjugated system can vary between two extreme resonance formulae (Scheme 2): a non-polar

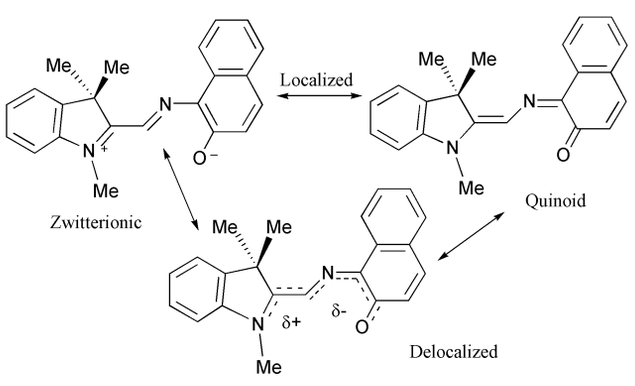


**Scheme 2**

quinoidal structure, which dominates in solvents of low polarity, and a zwitterionic structure, which becomes increasingly stable in polar media.[28] The electronic structure of merocyanine, either quinoid or zwitterionic, has been much discussed. Following a spectroscopic study, which revealed positive solvatochromic behaviour in the spirooxazine series, it was proposed that the structure is more quinoidal than zwitterionic.[29]

We performed Hartree–Fock and DFT calculations on the CTC merocyanine isomer using the 3-21G and 6-31G(d) basis sets. The main geometric parameters are listed in Table 3. Clearly, restricted Hartree–Fock (RHF) geometry optimization using the 3-21G and 6-31G(d) basis sets provides a quinoidal geometry as indicated by the C2–C2′, N1′–C11′ and C12′–O4′ double bond lengths. It should be noted that using a larger basis set does not dramatically change the geometry of the conjugated chain. However, instability calculation reveals that the RHF wavefunction suffers from RHF⟶UHF instability and unrestricted Hartree–Fock (UHF) calculations provide a zwitterionic geometry which is 20–25.5 kcal mol$^{-1}$ more stable than the RHF one. Inspection of the main geometric parameters calculated at the DFT level (Table 3) indicates that the merocyanine structure is between quinoidal and zwitterionic, and can be considered as delocalized (Scheme 2). Note that restricted as well as unrestricted DFT (UDFT) give exactly the same results. Clearly, DFT calculations give an average geometry between the quinoidal and zwitterionic formulae and, thus, are well suited for such compounds. Indeed, we have shown recently that the inclusion of correlation effects through DFT calculations on several classes of merocyanine products gives a more delocalized structure, while Hartree–Fock calculations give a more quinoidal one.[30]

s-*cis* Isomers are highly non-planar, as indicated by the *α*, *β* and *γ* dihedral angles (Fig. 1). The CCC and TCC isomers are more stable than the other s-*cis* isomers (CCT and TCT) because of the existence of a long range electrostatic attraction between the partially negatively charged O4′ oxygen (−0.533 e, Mulliken analysis at the DFT level) and positively charged C2 atom (0.511 e).

### 3.2 Interconversion between the coloured *trans* merocyanine forms

A large number of hypotheses have been proposed for the isomer distribution of photomerocyanines in different solvents. However, recent NMR[27] and picosecond time-resolved Raman spectroscopic studies[13] have firmly established that a significant amount of at least two isomers, TTC and CTC, exists in polar solvents. The purpose of this section is to calculate the energy barrier of interconversion of various s-*trans* isomers (Scheme 3), attempting to highlight the question of the number and the stability of the photomerocyanine isomers.

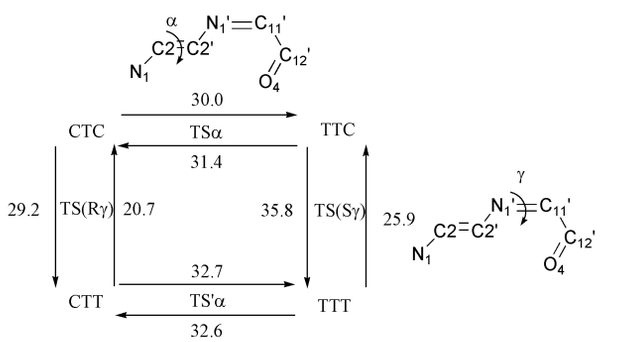


**Scheme 3** Interconversion of merocyanines (s-*trans*) isomers (*β* = 180°). The activation barriers (kcal mol$^{-1}$) are calculated at the B3LYP/6-31G(d)//3-21G level.

**Table 3** Selected parameters (in Å) for the CTC isomer calculated at different levels of theory [HF/3-21G, HF/6-31G(d), UHF/3-21G, UHF/6-31G(d), B3LYP/3-21G and B3LYP/6-31G(d)]

| Method | N1–C2 | C2–C2′ | C2′–N1′ | N1′–C11′ | C11′–C12′ | C12′–O4′ | $\mu$/D |
|---|---|---|---|---|---|---|---|
| HF/3-21G[a] | 1.366 | 1.351 | 1.374 | 1.283 | 1.488 | 1.227 | 2.94 |
| HF/6-31G(d)[b] | 1.366 | 1.355 | 1.368 | 1.276 | 1.508 | 1.203 | 2.79 |
| UHF/3-21G[c] | 1.383 | 1.367 | 1.358 | 1.349 | 1.453 | 1.289 | 1.58 |
| UHF/6-31G(d)[d] | 1.379 | 1.378 | 1.342 | 1.342 | 1.479 | 1.234 | 1.95 |
| B3LYP/3-21G[e] | 1.372 | 1.378 | 1.364 | 1.325 | 1.486 | 1.262 | 4.21 |
| B3LYP/6-31G(d)[f] | 1.368 | 1.385 | 1.351 | 1.321 | 1.496 | 1.241 | 4.30 |

[p] The atom numbering is shown in Scheme 1. [a] $E = -1022.76141088$ hartree. [b] $E = -1028.48861168$ hartree. [c] $E = -1022.80212860$ hartree. [d] $E = -1028.52267934$ hartree. [e] $E = -1029.42980403$ hartree. [f] $E = -1035.10769109$ hartree.

Since merocyanines have a *trans* configuration about the C2′–N1′ central bond, interconversion between the coloured isomers can only be achieved through rotation around the C2–C2′ bond ($\alpha$ rotation) or N1′–C11′ bond ($\gamma$ rotation). The $\alpha$ rotation connects the TTC and CTC or the TTT and CTT isomers. Rotation through the $\alpha$ dihedral angle is associated with a barrier of 30 kcal mol$^{-1}$ in the gas phase. The transition state geometries (TSα and TS′α) show a perpendicular arrangement of the indoline and naphthalene moieties (Fig. 2) and have a larger dipole moment (10.09 D) than photomerocyanines. Thus, a more polar environment should decrease the energy barrier to bond rotation. For example, the barrier calculated for the TTC⟶CTC reaction is 23 kcal mol$^{-1}$ in ethanol. Thermal conversion between merocyanines appears to be possible in polar solvents and equilibrium between coloured isomers could be established.

Isomerization around the N1′–C11′ bond ($\gamma$ rotation) is intrinsically more complicated since the process can be accomplished by two linearly independent kinds of motion, namely in-plane inversion at the nitrogen atom N1′ and rotation about the carbon–nitrogen bond[31] (Scheme 4).

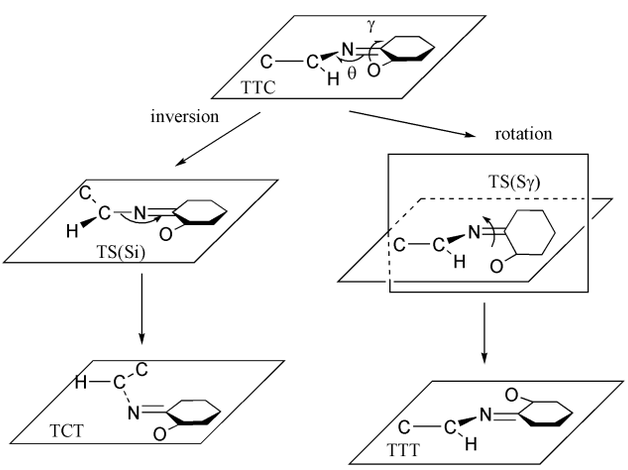


**Scheme 4** Interconversion involving the N1′=C11′ bond. Starting from the TTC configuration, the two isomers obtained by inversion (i) and rotation ($\gamma$) are TCT and TTT, respectively.

Starting from TTC, the three previous reactions lead to the TCT [in-plane inversion through the transition state TS(Si)], TTT [C1′–N11′ bond rotation, TS(Sγ)] isomers. In the same way, the similar transition states of inversion obtained from the TTT, CTC and CTT isomers are named TS(S′i), TS(Ri) and TS(R′i), respectively (Table 4). In spite of extensive search, no rotational transition structure, TS(Sγ), was located on the potential energy surface at the B3LYP/3-21G level of calculation. When complete optimization was carried out, the structure collapsed toward a linear C2′–N1′–C11′ geometry, corresponding to an inversion mechanism. To overcome this difficulty, the transition state for rotation about the N1′–C11′ bond was approximated by freezing the C2′–N1′–C11′ angle at a value of 130°. Under this approximation, and considering the TTC↔TTT reaction, the optimized transition states TS(Sγ) lie 35.8 kcal mol$^{-1}$ above the TTC and 25.9 kcal mol$^{-1}$ above the TTT isomers (Scheme 3). One can consider that the thermal equilibrium between TTC and TTT is almost completely shifted towards TTC. The dipole moments of the transition state and TTT are 5.8 and 5.4 D, respectively. Therefore, only a small stabilization of the transition state with respect to the reactant and product is expected in polar solvents. Similar behaviour is found for the CTC↔CTT reaction [TS(Rγ) transition state]. On the basis of these calculations, it can be concluded that only the interconversion reactions involving the C2–C2′ bond are possible in polar solvents and in both directions between the TTC and CTC isomers, while reactions involving rotation about the N1′–C11′ bond are possible only in the TTT⟶TTC and CTT⟶CTC directions.

### 3.3 Ring-closure reactions of the merocyanine forms

In this section, we describe the four ring-closure reactions starting from the TTC, CTT, TTT and CTC isomers. The energies of the transition states located along the different pathways are listed in Table 4 and their geometries displayed in Fig. 2.

It was previously established that the thermal fading relaxation kinetics in the spirooxazine series exhibit two phases: a slow one (relaxation time 0.5–10 s) and a fast one (relaxation time 5–50 ms).[29,32] These results indicate that the ring-closure reaction could involve, at least, two different merocyanine isomers. The conversion from merocyanine to spirooxazine involves rotation about each bond of the central conjugated chain. By analogy with the cyclohexatriene ring closing, as previous envisaged for the pyran model,[33] two pathways can be considered. The first, labeled (**a**), requires two steps: a *trans–cis* isomerization about the central C2′–N1′ bond followed by C–O bond formation to give the closed spiro form. These pathways connect CTC with CF(R) and TTC with CF(S) (paths **Ra** and **Sa**, Scheme 5). The second pathway, labeled (**b**), requires three

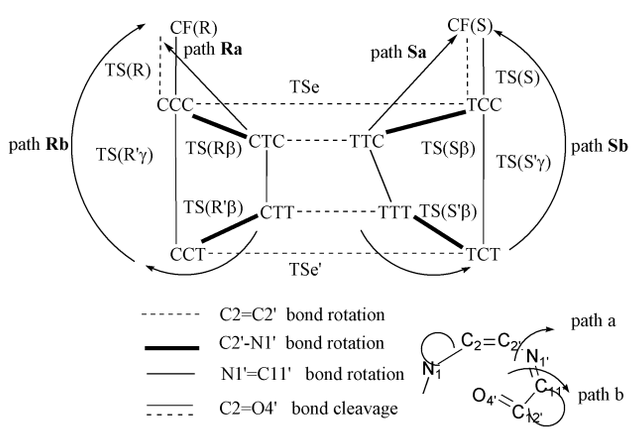


**Scheme 5** General scheme for isomerizations and ring-closure reactions (paths **a** and **b**) of the central conjugated chain.

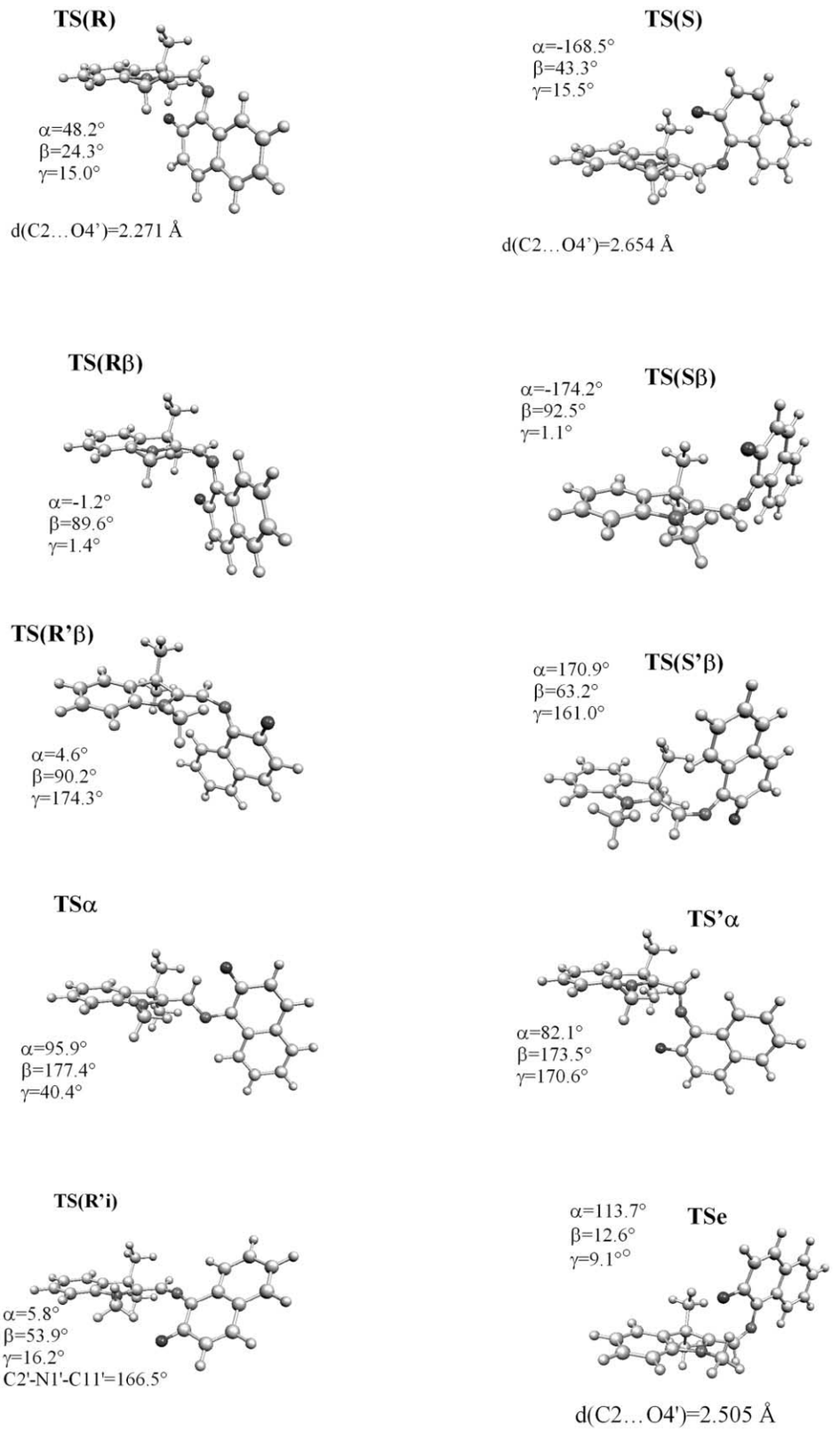


**Fig. 2** B3LYP/3-21G optimized geometries of ground transition states located along the ring opening/closing reactions connecting CF(R) with CTC and CTT (left, path **Ra** and **Rb**) and CF(S) with TTC and TTT (right, path **Sa** and **Sb**). between CTC and TTC (TSα), CTT and TTT (TS′α), CCC and TCC (TSe), and transition of inversion between CTT and CCC [TS(R′i)].

steps: two bond rotations around the C2′–N1′ and N1′–C11′ bonds and C–O bond formation. For example, starting from CTT the sequential reactions leading to CF(R) are: CTT⟶ CCT⟶CCC⟶CF(R) (path **Rb**, Scheme 5).

**3.3.1. Ring-closure reactions from the most stable isomers, TTC and CTC.** As previously noted, recent NMR and resonance Raman studies have shown unambiguously that the TTC and CTC isomers are the most stable photomerocyanines formed during the photochromism process.[13,27] We therefore first focused our attention on the ring-closure reaction from these isomers leading to the corresponding closed forms, CF(R) and CF(S), respectively (paths **Ra** and **Sa**, Scheme 5). The optimized transition states located along these pathways are depicted in Fig. 2. Schematic potential energy profiles of the **Ra** and **Sa** pathways are displayed in Fig. 3.

**Table 4** Calculated relative energies, $\Delta E$/kcal mol$^{-1}$, of the ground state transition states (B3LYP/3-21G//3-21G and B3LYP/6-31G(d)//3-21G)

| Transition state | Connected species | B3LYP/3-21G $\Delta E^a$ | B3LYP/6-31G(d)//3-21G $\Delta E^a$ | B3LYP/6-31G(d)//3-21G $\Delta G_{solvation}$ |
|---|---|---|---|---|
| TS(R) | CF(R)↔CCC | 19.8 | 17.8 | −5.4 |
| TS(S) | CF(S)↔TCC | 26.0 | 22.1 | −5.2 |
| TS(Rβ) | CCC↔CTC | 29.8 | 25.0 | −4.7 |
| TS(Sβ) | TCC↔TTC | 29.2 | 24.5 | −5.3 |
| TS(R′β) | CTT↔CCT | 34.4 | 28.1 | −5.9 |
| TS(S′β) | TTT↔TCT | 34.7 | 29.3 | −5.9 |
| TS(Rγ) | CTC↔CTT | 43.6 | 33.3 | −6.6 |
| TS(Sγ) | TTC↔TTT | 42.4 | 38.6 | −6.7 |
| TS(R′γ) | CCT↔CCC | 53.7 | 48.8 | −7.7 |
| TS(S′γ) | TCT↔TCC | 58.9 | 52.4 | −11.0 |
| TS(Ri) | CTC↔CCT | 38.0 | 33.3 | −6.1 |
| TS(Si) | TTC↔TCT | 41.1 | 36.2 | −6.7 |
| TS(R′i) | CTT↔CCC | 30.4 | 30.0 | −3.08 |
| TS(S′i) | TTT↔TCC | 28.3 | 28.7 | −4.1 |
| TSα | TTC↔CTC | 38.2 | 34.1 | −11.6 |
| TS′α | TTT↔CTT | 50.8 | 45.3 | −11.3 |
| TSe | TCC↔CCC | 28.7 | 26.5 | −7.5 |

[a] Energy relative to CF(R).

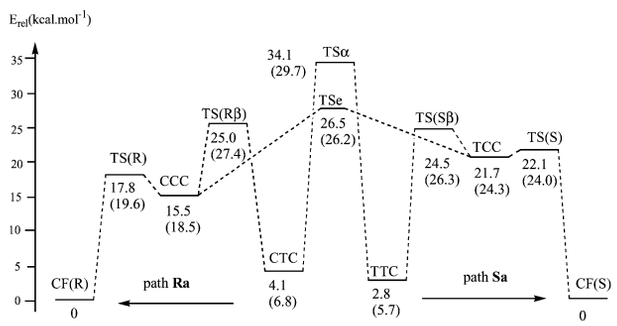


**Fig. 3** Ground state adiabatic potential energy profit (path **a**) for the pathways of ring-opening/closing **Ra** and **Sa**. Relative energies are in kcal mol$^{-1}$ [B3LYP/6-31G(d)//3-21G in the gas phase and in ethanol in brackets].

Beginning with one of the most stable *trans*-merocyanine, CTC, the ring-closure pathway, **Ra**, contains two transition states, TS(Rβ) and TS(R), and one intermediate, CCC. The first step in the ring-closure reaction changes the planar geometry to a perpendicular geometry by rotation about the central C2′–N1′ bond in the transition state TS(Rβ) (Fig. 2, the reaction coordinate is mainly the $\beta$ dihedral angle). In these transition geometries, the molecule has two non-interacting π-conjugated systems: one involves the indolinic moiety while the second implies conjugation of the lone pair of the N1′ atom with the naphthalene part. Further rotation about C2′–N1′ bond leads to the s-*cis* isomers CCC previously described. The second stage of this two-step mechanism connects the s-*cis* intermediates with the closed forms through the transition state of C2′–O4′ bond formation, TS(R). The TS(R) transition states both have a six-membered-ring structure (Fig. 2) and the O4′–C2 bond length is 2.27 Å. Similar values for C–C bond formation in transition states have been obtained for a large number of pericyclic reactions.[34] Inspection of the dihedral angles $\alpha$, $\beta$ and $\gamma$ indicates that this TS does not retain the perpendicular geometry of the parent closed molecule and the two conjugated moieties (indolinic and naphthalene moieties) deviate by an angle of *ca.* 20° from the orthogonal arrangement (Fig. 2). From an energetic point of view, the most significant result from the calculations is that the *cis–trans* isomerization (C2′–N1′ bond rotation) has the highest barrier of the overall ring-closure reaction (20.9 kcal mol$^{-1}$ in the gas phase calculations, Fig. 3). This result stands in contrast to those of previous *ab initio* calculations, performed at the Hartree–Fock level and undertaken on the spiropyran ring-closure reaction,[11] in which C–O bond formation was found to be the rate-determining step. Probably, the discrepancy comes from the quinoidal description at the Hartree–Fock level of the merocyanine which provides a single central bond instead of partial double bond character. As a consequence, the *cis–trans* isomerization is found to occur without an energy barrier. Quite similar results are obtained for the ground state ring-closure reaction starting from the TTC isomer: the activation barrier for the rate-determining step is calculated to be 21.7 kcal mol$^{-1}$.

Our results suggest that the thermal ring-closure rates for the two most stable open forms, CTC and TTC, are approximately the same within the accuracy of the quantum chemical calculations used here. On this basis, the origin of the second kinetic phase observed for the thermal fading of spirooxazine remains unclear. Since neither a fully established equilibrium between the s-*trans*-merocyanines nor the ring-closure reactions of TTC and CTC are able to explain the biexponential kinetics, we turned toward the study of the ring-closure pathways starting instead from the two other, less stable, s-*trans* isomers CTT and TTT (paths **Rb** and **Sb**).

**3.3.2. Ring-closure reactions from the less stable isomers, TTT and CTT.** The calculated energy profiles of the ring-closure reactions of CTT and TTT are shown in Fig. 4. Starting from CTT and TTT, the first C2′–N1′ rotation is achieved *via*

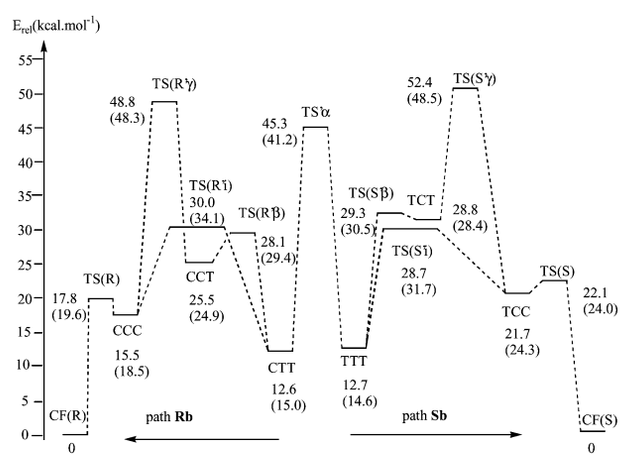


**Fig. 4** Ground state adiabatic potential energy profile (path **b**) for the pathways of ring-opening/closing **Rb** and **Sb**. Relative energies are in kcal mol$^{-1}$ [B3LYP/6-31G(d)//3-21G in the gas phase and in ethanol in brackets].

TS(R′β) and TS(S′β) (see the optimized geometries in Fig. 2) to give the high-energy s-*cis* isomers, CCT and TCT, respectively (Table 1). The CCT and TCT isomers are connected to the CCC and TCC isomers through TS(R′γ) and TS(S′γ), which are located at *ca.* 48.8 and 48.5 kcal mol$^{-1}$ above the closed forms. Clearly, the second step (CCT⟶CCC or TCT⟶TCC) of these mechanisms is rate-determining (Fig. 4) and makes the ring closure of TTT and CTT energetically more difficult that of CTC and TTC. This result suggests, at this stage of the study, that the ring-closure reactions from the less stable merocyanine isomers (TTT and CTT) are slower than those from the more stable ones (TTC and CTC). For instance, the energy barriers for ring closure are calculated to be 36.2 and 35.8 kcal mol$^{-1}$ for CTT⟶CF(R) and TTT⟶CF(S), respectively. This result seems to be in contradiction with chemical sense, which suggests that the less stable the open form, the faster is the ring closure. However, an alternative and more favorable mechanism of back reversion may be envisaged for these CTT and TTT isomers. For instance, the s-*trans* CTT isomer can reach the CCC s-*cis* intermediate directly through the transition state for inversion at the nitrogen N1′ atom, TS(R′i), showing as expected a linear C2′–N1′–C11′ geometry (Fig. 2). The CTT⟶CCC barrier for inversion is found to be considerably less than that for the bond rotation mechanism (17.4 *vs.* 36.2 kcal mol$^{-1}$). The behaviour is very similar for the transformation of TTT to TCC involving N1′-inversion *via* the TS(S′i) transition state. Consequently, from the CTT and TTT isomers, the isomerization reactions necessary for ring closure prior to C–O bond formation are likely to occur by inversion instead of double bond rotation. Moreover, it can be seen that the energy barriers for these mechanisms are in the range 15–20 kcal mol$^{-1}$, which is somewhat lower than the barrier for ring closure from the TTC and CTC isomers. Therefore, it is suggested that the fast component observed in the kinetic reaction could originate from an inversion starting from the CTT and TTT isomers rather than from a slower double bond rotation.

### 3.4 Ring-opening and enantiomerization reaction

The spirooxazine studied also exhibits weak thermochromism in ethanol but not in non-polar solvents. The first step of the thermochromic reaction involves cleavage of the O4′–C2 bond from the closed forms through the TS(R) and TS(S) transition states. It should be noted that the transition states of C–O bond cleavage, TS(R) and TS(S), exhibit ionic character with partial negative charge on the oxygen and a partial positive charge on the C2′ carbon atoms. This result establishes that the opening reaction is a heterolytic rather than a homolytic process.[35] The marked difference between the **Ra** and **Sa** routes is that the C–O bond cleavage in the latter requires more energy (22.1 kcal mol$^{-1}$ in the gas phase and 24.0 kcal mol$^{-1}$ in ethanol) than in the former (17.8 kcal mol$^{-1}$ in the gas phase and 19.6 kcal mol$^{-1}$ in ethanol). This result is consistent with the Hammond[36] postulate and higher late character for TS(S). Comparison of the C–O bond-breaking energy with experiment is difficult because in most experimental studies the C–O bond-breaking step is considered to be the rate-determining step of the thermochromic reaction. Clearly, this is not the case from our calculations. The pathway involves rotation about the central C2′–N1′ and connects the s-*cis* intermediates CCC or TCC with the corresponding coloured photomerocyanines CTC or TTC through TS(Rβ) and TS(Sβ), which are located above TS(R) and TS(S). The reaction of colouration is controlled by the *cis–trans* reaction and the energy barrier is calculated to be about 25 kcal mol$^{-1}$ in the gas phase and 26 kcal mol$^{-1}$ in ethanol. Comparison with experimental values shows better agreement with the ethanol value (24.4 kcal mol$^{-1}$ in ethanol[25]). Considering now the enantiomerization reaction of the closed forms CF(R) and CF(S), two pathways may be envisaged. The most favorable pathway connects, after C–O bond breaking, the two s-*cis* forms, CCC and TCC. A transition state, labeled TSe, between CCC and TCC was located on the PES (Fig. 2). The activation barrier of this reaction is predicted to be 26.5 kcal mol$^{-1}$. Assuming that enantiomerization between CF(R) and CF(S) follows this route, one can note that this reaction does not involve coloured forms. The second pathway for enantiomerization was calculated to be less favorable, requiring first the formation of coloured merocyanine isomers TTC and CTC, and isomerization through the TSα transition state (Fig. 2). The rate-determining step of this last pathway is the *trans–trans* reaction (TTC⟶CTC) with a barrier of 31.3 kcal mol$^{-1}$. Clearly, the calculations provide strong support for an enantiomerization reaction in the absence of any observable colour change, which is in fair agreement with experiments on related compounds.[9]

## 4 Conclusion

The thermal colouration and decolouration of a spirooxazine were studied by performing DFT calculations. All feasible reactions of ring closure as well as isomerization between merocyanine isomers have been calculated and add support to the assignment of the experimental data.

The mechanisms of ring closure from the four merocyanine isomers have been determined. Each of the ring-closure reactions involves two steps (merocyanine⟶s-*cis* isomerization followed by C–O bond formation) which suggests that the kinetics could have two phases. However, calculations indicate that the s-*cis*⟶CF reaction occurs with a very low barrier. The ratio of the rate constants calculated within the approximation of the Arrhenius law indicate that the second step is $10^{11}$ to $10^{15}$ times faster than *cis–trans* isomerization and in these conditions the kinetics of thermal fading should be monoexponential. We carefully considered the ring-closure reactions of the CTC and TTC isomers. The barrier to *cis–trans* isomerization, *i.e.* the rate-determining step, is calculated to be the same for both reactions, which suggests that these isomers have the same rate of ring closure. The less stable merocyanine isomers, CTT and TTT, revert back to the corresponding closed forms through an inversion mechanism at the nitrogen atom, and the rate of this process is probably faster than that of *cis–trans* isomerization about the central C–N bond [TS(R′i) and TS(S′i) are more stable than TS(Rβ) and TS(Sβ)]. Therefore, the CTT and TTT isomers should revert to the closed form faster than the CTC and TTC isomers. This result could explain the fast component of the thermal fading kinetics. It should be noted that the energy barriers for ring closure of the CTT and TTT isomers are slightly different and therefore, in principle, two fast kinetics of thermal fading could be observed. Finally, if we assume that four merocyanines are produced through primary processes and that isomerization reactions between these isomers are not possible (in a non-polar solvent), three different kinetics (one slow and two fast) should be observed for thermal back reaction. In a polar solvent, the energy barrier for isomerization of merocyanines is lowered, and CTT and TTT can isomerize to the CTC and TTC isomers, respectively. These isomerization reactions are energetically more favorable than the ring closure ones and, finally, the thermal decolouration comes only from the ring closure of the TTC and CTC isomers. As a consequence, in polar solvents, the fast component of the kinetic relaxation could disappear and only the slow kinetics would remain. It should be noted that this interpretation is qualitatively in agreement with the experimental results obtained on such compound in this series.

Finally, we showed that the racemization between the enantiomeric closed forms CF(R) and CF(S) requires an interconversion of two s-*cis* intermediates, CCC and TCC, and thus does not involve coloured forms. This result is in agreement with experiment.

## References


1 R. C. Bertelson, in *Photochromism*, ed. G. H. Brown, Techniques in Chemistry, Wiley-Interscience, New York, 1971, Vol. 3, p. 45; *Photochromism: Molecules & Systems*, ed. H. Durr and H. Bouas-Laurent, Elsevier, New York, 1990.

2 *Organic Photochromic and Thermochromic Compounds*, ed. J. C. Crano and R. J. Guglielmetti, Kluwer Academic/Plenum Publishers, New York, 1999.

3 N. Y. C. Chu, in *Photochromism: Molecules & Systems*, ed. H. Durr and H. Bouas-Laurent, Elsevier, New York, 1990, p. 493.

4 S. Maeda, *Organic Photochromic and Thermochromic Compounds*, ed. J. C. Crano and R. J. Guglielmetti, Kluwer Academic/Plenum Publishers, New York, 1999, Vol. 1, pp. 85–109.

5 J. C. Crano, W. S. Kwak and C. N. Welch, *Applied Photochromic Polymer Systems*, ed. C. B. McArdle, Blackie, London, 1992, ch. 2, p. 31.

6 G. Berkovic, V. Krongauz and V. Weiss, *Chem. Rev.*, 2000, **100**, 1741.

7 A. Samat and V. Lokshin, *Organic Photochromic and Thermochromic Compounds*, ed. J. C. Crano and R. J. Guglielmetti, Kluwer Academic/Plenum Publishers, New York, 1999, Vol. 2, p. 415.

8 E. Pottier, R. Dubest, R. Guglielmetti, P. Tardieu, A. Kellmann, F. Tfibel, P. Levoir and J. Aubard, *Helv. Chim. Acta*, 1990, **73**, 303.

9 R. Kiesswetter, N. Pustet and A. Mannschreck, *Tetrahedron: Asymmetry*, 1999, **10**, 4677; A. Mannschreck, L. Lorenz and M. Schinabeck, *Organic Photochromic and Thermochromic Compounds*, ed. J. C. Crano and R. J. Guglielmetti, Kluwer Academic/Plenum Publishers, New York, 1999, Vol. 2, pp. 261–295.

10 J. D. Stewart, L. J. Liotta and S. J. Benkovic, *Acc. Chem. Res.*, 1993, **26**, 396.

11 P. N. Day, Z. Wang and R. Pachter, *J. Phys. Chem.*, 1995, **99**, 9730.

12 S. Nakamura, K. Uchida, A. Murakami and M. Irie, *J. Org. Chem.*, 1993, **58**, 5543.

13 J. Aubard, F. Maurel, G. Buntinx, R. Guglielmetti and G. Lévi, *Mol. Cryst. Liq. Cryst.*, 2000, **345**, 203.

14 C. W. Bauschlicher, *Chem. Phys. Lett.*, 1995, **246**, 40; A. A. El-Azhary and H. U. Suter, *J. Phys. Chem.*, 1996, **100**, 15056.

15 C. Lee, W. Yang and R. Parr, *Phys. Rev. B*, 1988, **37**, 785; A. D. Becke, *J. Chem. Phys.*, 1993, **98**, 5648.

16 J. S. Binkley, J. A. Pople and W. J. Hehre, *J. Am. Chem. Soc.*, 1980, **102**, 939.

17 M. J. Frisch, G. W. Trucks, H. B. Schlegel, P. M. W. Gill, B. G. Johnson, M. A. Robb, J. R. Cheeseman, T. Keith, G. A. Petersson, J. A. Montgomery, K. Raghavachari, M. A. Al-Laham, V. G. Zakrzewski, J. V. Ortiz, J. B. Foresman, J. Cioslowski, B. B. Stefanov, A. Nanayakkara, M. Challacombe, C. Y. Peng, P. Y. Ayala, W. Chen, M. W. Wong, J. L. Andres, E. S. Replogle, R. Gomperts, R. L. Martin, D. J. Fox, J. S. Binkley, D. J. Defrees, J. Baker, J. P. Stewart, M. Head-Gordon, C. Gonzalez and J. A. Pople, Gaussian 94, Revision E.1, Gaussian, Inc., Pittsburgh, PA, 1995.

18 P. C. Hariharan and J. A. Pople, *Chem. Phys. Lett.*, 1972, **66**, 217; W. J. Hehre L. Radom, P. v. R. Schleyer and J. A. Pople, *Ab Initio Molecular Orbital Theory*, Wiley, New York, 1986.

19 S. Miertus and E. Scrocco Tomasi, *J. Chem. Phys.*, 1981, **55**, 117.

20 K. Fukui, *J. Phys. Chem.*, 1970, **44**, 4161; K. Fukui, *Acc. Chem. Res.*, 1981, **14**, 363.

21 V. R. Jensen, K. J. Borve and M. Ystenes, *J. Am. Chem. Soc.*, 1995, **117**, 4109; L. Deng and T. Ziegler, *J. Phys. Chem.*, 1995, **99**, 612.

22 R. Millini, G. Del Piero, P. Allegrini, L. Crisci and V. Malatesta, *Acta Crystallogr., Sect. C: Cryst. Struct. Commun.*, 1991, **47**, 2567.

23 A. Aldoshin, *Organic Photochromic and Thermochromic Compounds*, ed. J. C. Crano and R. J. Guglielmetti, Kluwer Academic/Plenum Publishers, New York, 1999, Vol. 2, pp. 297–355.

24 N. P. Ernsting and Th. Arthen-Engeland, *J. Phys. Chem.*, 1991, **95**, 5502.

25 G. Favaro, F. Masetti, U. Mazzucato and G. Ottavi, *J. Chem. Soc., Faraday Trans.*, 1994, **90**, 333.

26 H. Takahashi, K. Yoda, H. Isaka, T. Ozechi and Y. Sakaino, *Chem. Phys. Lett.*, 1987, **140**, 90.

27 S. Delbaere, C. Bochu, N. Azaroual, G. Buntinx and G. Vermeersch, *J. Chem. Soc., Perkin Trans. 2*, 1997, 1499.

28 C. Reichardt, *Solvents and Solvent Effects in Organic Chemistry*, 2nd edn., VCH, Weinheim, 1988, p. 298.

29 A. Kellmann, F. Tfibel, R. Dubest, P. Levoir, J. Aubard, E. Pottier and R. Guglielmetti, *J. Photochem. Photobiol., A*, 1989, **49**, 63.

30 F. Maurel, A. Samat, R. Guglielmetti and J. Aubard, *Mol. Cryst. Liq. Cryst.*, 2000, **345**, 75.

31 V. Bonacic-Koutecky and J. Michl, *Theor. Chim. Acta*, 1985, **68**, 45; T. Asano, H. Furuta, H.-J. Hofmann, R. Cimiraglia, Y. Tsuno and M. Fujio, *J. Org. Chem.*, 1993, **58**, 4418; M. Pankratz and R. F. Childs, *J. Org. Chem.*, 1985, **50**, 4553.

32 A. K. Chibisov and H. Görner, *J. Phys. Chem. A*, 1999, **103**, 5211.

33 F. Zerbetto, S. Monti and G. Orlandi, *J. Chem. Soc., Faraday Trans. 2*, 1984, **80**, 1513.

34 K. N. Houk, Y. Li and J. D. Evanseck, *Angew. Chem., Int. Ed. Engl.*, 1992, **31**, 682.

35 Y. Sueishi and T. Nishimura, *J. Phys. Org. Chem.*, 1995, **8**, 335.

36 G. S. Hammond, *J. Am. Chem. Soc.*, 1955, **77**, 334.